Pure & Appl. Chem., Vol. 48, pp. 77–97. Pergamon Press, 1976. Printed in Great Britain.

ELECTRON SPECTROSCOPY AND MOLECULAR STRUCTURE

KAI SIEGBAHN
Institute of Physics, Uppsala University, Box 530, S-75121, Uppsala, Sweden

Abstract—Electron spectroscopy can now be applied to solids, liquids and gases. Some fields of research require ultrahigh vacuum conditions, in particular those directly concerned with surface phenomena on the monolayer level. Liquids have recently been subject to studies and several improvements and extensions of this technique can be done. Much advance has lately been achieved in the case of gases, where the pressure range presently is $10^{-5} - 1$ torr. Signal-to-background ratios for core lines can be ~ 1000:1 and the resolution has been increased to the extent that vibrational fine structures of 1s levels in some small molecules have been observed. These improvements are based on the monochromatization of the exciting AlK_α radiation. Under such conditions the background is so much reduced that shake-up structures are more generally accessible for closer studies. ESCA shifts are also much easier to resolve and to measure with higher precision around 0.02 eV. It is interesting to compare the results from electron spectroscopy with those recently obtained from X-ray emission spectra of free molecules. By means of grating at grazing incidence a resolution has been obtained at a sufficient intensity to record not only transitions from resolved molecular orbitals to the 1s levels but also in some cases vibrational fine-structures inside such separate lines.

The photoionization dynamics including atomic and molecular relaxations have been investigated, both experimentally and theoretically. In the valence electron region improvements in energy resolution and in the application of the intensity model based on the MO-LCAO approximation greatly facilitate the assignments of the valence orbitals. Accumulation of empirical evidences gathered from series of similar chemical species and also better methods of calculation, both ab initio and semi-empirical, have gradually resulted in a much better understanding of the molecular orbital description.

The experience of the latest ESCA instrument with monochromatization has motivated an attempt to design an optimized apparatus according to the general principles of this prototype. A considerable gain in intensity can be made at an improved resolution set by the inherent diffraction pattern of the focussing spherical quartz crystals.

INTRODUCTION

Electron spectroscopy has been reviewed several times during the last years and more recently by the author in the conference volume[1] of the *Namur Conference on Electron Spectroscopy* (1974). The reader is referred to this book for a more complete account of the present situation in the field and to a comprehensive list of references. In the following I will briefly summarize first some features of this spectroscopy and then illustrate with some recent applications, some of which have not yet been published.

Electron spectroscopy was originally started in my laboratory for precise measurements of electron binding energies in atomic and solid state physics. After some ten years development work it gradually became clear that this spectroscopy should have interesting applications in chemistry. With this conclusion in mind the acronym ESCA, Electron Spectroscopy for Chemical Analysis, was coined around 1965. The word Analysis was then taken in a more modern and broader sense than the classical one. For example, one very important application of ESCA is surface analysis. One can analyze both solids, gases and, more recently, liquids. All elements, including the important light elements carbon, nitrogen and oxygen, can be analysed on the surface with high accuracy. A particular feature of ESCA is that in addition to the elemental composition of a compound frequently other useful information can be obtained about the chemical bonds and charge distribution. This information can be deduced from the so-called ESCA shifts of the core level electron lines. When atoms are brought close together to form a molecule the electron orbitals of each atom are perturbed. Inner orbitals, that is, those with higher binding energies, may still be regarded as atomic and belonging to specified atoms within the molecule, whereas the outer orbitals combine to form the valence level system of the molecule. These orbitals play a more or less active part in the chemical bonds which are formed between the atoms in the molecule and which define the chemical properties. The chemical bonds affect the charge distribution so that the original neutral atoms can be regarded as charged to various degrees while the neutral molecule retains a net charge of zero. One may describe the situation by regarding the individual atoms in the molecule as spheres with different charges set up by the transfer of certain small charges from one atomic sphere to the neighbouring atoms taking part in the chemical bond. Inside each charged sphere the atomic potential is constant in accordance with classical electrostatic theory. The result of this atomic potential is to shift the whole system of inner levels in a specified atom by a small amount, the same for each level. Levels belonging to different atoms in the molecule are generally shifted differently, however, and by measuring these ESCA "chemical shifts" for individual atoms in the molecule a mapping can be made of the distribution of charge or potential in the molecule. This is then a reflection of the chemical bondings between the atoms which in turn can be described by the orbitals in the valence level system. It should be remarked that these chemical shifts are different from those obtained in NMR and may even go in the reverse direction.

The chemical shift effect has its theoretical importance in the study of molecular electronic structure. In other contexts its usefulness lies precisely in its ability to specify the chemical composition, in particular at sur-

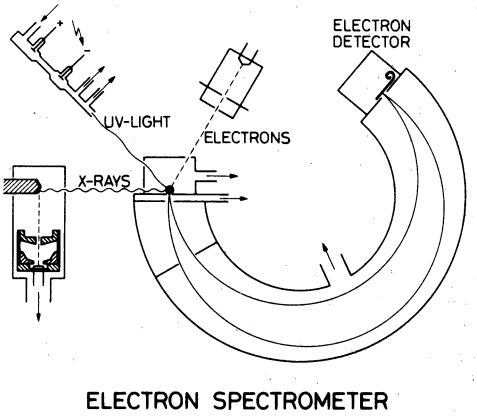

Fig. 1. Excitation of electron spectra by three different modes.

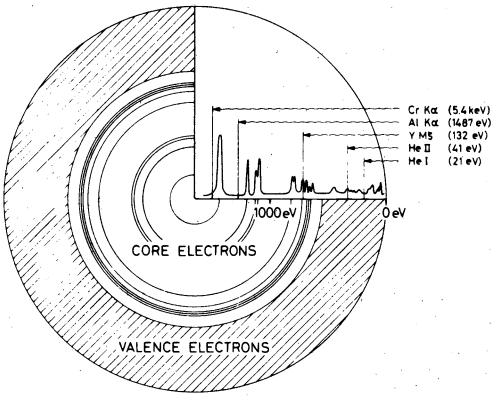

Fig. 2. Excitation of core and valence electron lines at various photon energies.

faces. For example, a metal and its oxide give two distinctly different lines because of the chemical shift effect. It is therefore often easy to follow the rate of oxidation at a surface or the removal of an adsorbed gas layer from it. The chemical composition of a surface or the changes due to various chemical or physical treatments are amenable to detailed examination.

MODES OF EXCITATION

Electron spectra can be excited in three different ways (Fig. 1): by means of X-rays (for example AlK_α at 1487 eV, or $YM\zeta$ at 132 eV) UV-light (usually the He resonance radiation at 21.22 eV or 40.8 eV) or an electron beam. The various modes of excitation generally provide complementary information. From X-rays and UV one obtains well defined photoelectron lines, whilst electrons produce Auger lines (and autoionization electron lines). Auger electron lines are also always obtained by means of X-rays. Figure 2 illustrates how photons of various wavelengths can excite electron spectra from different levels of an atom within a molecule. The binding energy region between 0–50 eV is usually classified as the valence electron region. These orbitals are more or less delocalized and can be excited by both X-rays and UV. The core region inside the valence region is atomic in character and is typical for a given element and therefore convenient for analytical purposes. This region can be reached by X-rays.

More recently, synchrotron radiation has been used to excite electron spectra (see Fig. 3). If a variable monochromator is inserted between the synchrotron and the electron spectrometer one can excite the different electron spectral energies in a continuous way. Since this radiation is linearly polarized in the direction of the plane of the accelerator one can also study the spectra as a function of the angle between the emitted electrons and

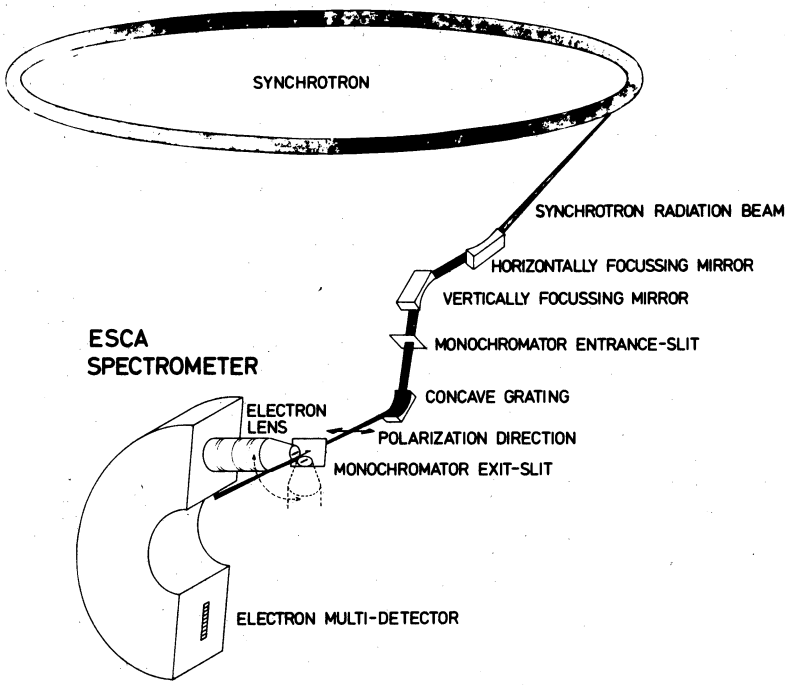

Fig. 3. Electron spectroscopy by means of synchrotron radiation as the source of excitation.

the electric vector of the radiation by turning the electron spectrometer in the photon beam.

Usually, it is sufficient to use only one energy of X-radiation. It is, however, highly desirable to monochromatize this radiation to an extent which is better than the inherent width of the main X-ray line itself. This can be done in different ways but common to them all is an X-ray dispersive element such as a bent quartz crystal. Figure 4 shows the principle of such a system. An electron gun yields a well focussed electron beam of high intensity impinging on the periphery of a swiftly rotating, water cooled anode F. Along the Rowland circle one or several spherically bent quartz crystals (Q) accept the AlK_α radiation at a small angle of emittance (~5°). Only the central part of the K_α line satisfies the diffraction conditions and this narrow wavelength region is reflected towards the slit of the sample chamber G. This chamber may contain a gas, liquid or a solid. The expelled electrons are partly transmitted through a narrow slit facing the electron spectrometer, and after passing a lens system, which can retard the electrons to a convenient energy, they are analyzed in a spherical electrode energy analyzer. Alternatively, a He lamp or a small electron gun can be used for excitation in the same arrangement. The electrons are focussed by the analyzer in its focal plane. Along this plane an extended electron detector is situated. This is a position sensitive device consisting of two electron channel plates close to each other, giving a total multiplication of 10^8. These multiplied electrons are further accelerated onto a phosphorus screen continuously observed and scanned by a TV camera. In this way the whole system works at maximum efficiency. All data are recorded and stored into a computer. The apparatus is shown in Fig. 5. An extensive pump system is required to provide the differential pumping which is necessary for handling gases and liquid samples.

EXAMPLES OF ELECTRON SPECTRA

Some examples may illustrate the kind of spectra one obtains in ESCA. We start with the gas phase of a droplet of mercury which is introduced into the sample chamber by means of a vacuum lock device in the instrument shown in Fig. 5.Already at room temperature the vapour pressure (10^{-3} torr or 10^{-1} Pa) is enough to produce the spectrum given in Fig. 6. This spectrum contains all the levels which can be excited by AlK_α, namely N_I, N_{II}, N_{III}, N_{IV}, N_V, N_{VI}, N_{VII} and O_I, O_{II}, O_{III}, O_{IV}, O_V and P_I. No selection rules discriminate against the appearance of the complete level systems. One can also observe some satellite structure behind the $N_{VI}N_{VII}$ lines. Figure 7 is a closer study of this structure in the vapour phase (upper figure) and the solid phase (lower figure). These spectra disclose some other typical features of ESCA, namely so-called shake-up lines (in the gas) and plasmon loss peaks (for the Hg metal). In addition to the former lines appearing in the gas phase, one can also observe some extra peaks due to external, discrete energy losses of the electrons originating from the $N_{VI}N_{VII}$ peaks, which occur when these electrons are traversing the gas before reaching the slit. All these electron lines give information about excited states in the residual ion or in the neutral molecule. Plasmon peaks are characteristic of mercury metal electron plasma.

It is interesting to look at the very last part of the Hg spectrum close to the binding energy zero (see Fig. 8) both for the gas (upper figure) and for the metal (lower figure). One clearly observes how the broadening of levels occurs at condensation when the free atoms combine to form a solid, the uttermost level P_I (or $6s_{1/2}$) thereby resulting in the broad conduction band with the Fermi edge. Conduction band spectra of all metals and their alloys can be studied in this way by ESCA.

Figures 9a and 9b show the conduction bands of gold and platinum. Osmium (Fig. 9d)[2] displays a number of features which can be compared to theoretical band calculations. One observes for the case of gold the s-band extending to the Fermi edge and furthermore the splitted d-band structure. The platinum has a very high density of states at the Fermi edge.

As mentioned, a special feature of ESCA is that by measuring the exact position of the electron lines characteristic of the various elements in the molecule, one can move the area of inspection from one atomic species to the other in the molecular structure. For example, one can observe one single iron atom and two disulfide bridges in a large biomolecule like cytochrome-c (mol. wt = 12,700),

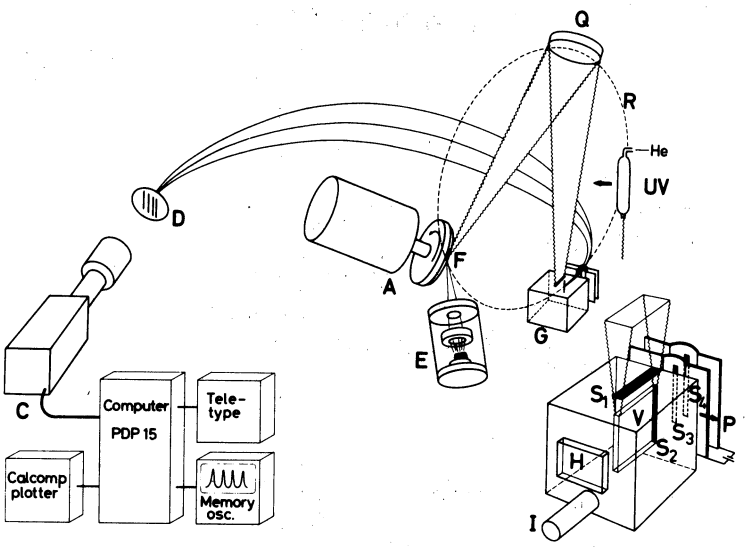

Fig. 4. The prototype ESCA instrument (1972) for gases and solids with monochromatized AlK_α radiation ($\Delta h\nu = 0.2$ eV).

Fig. 5. Photograph of the prototype ESCA instrument according to Fig. 4. For further developments see Fig. 42.

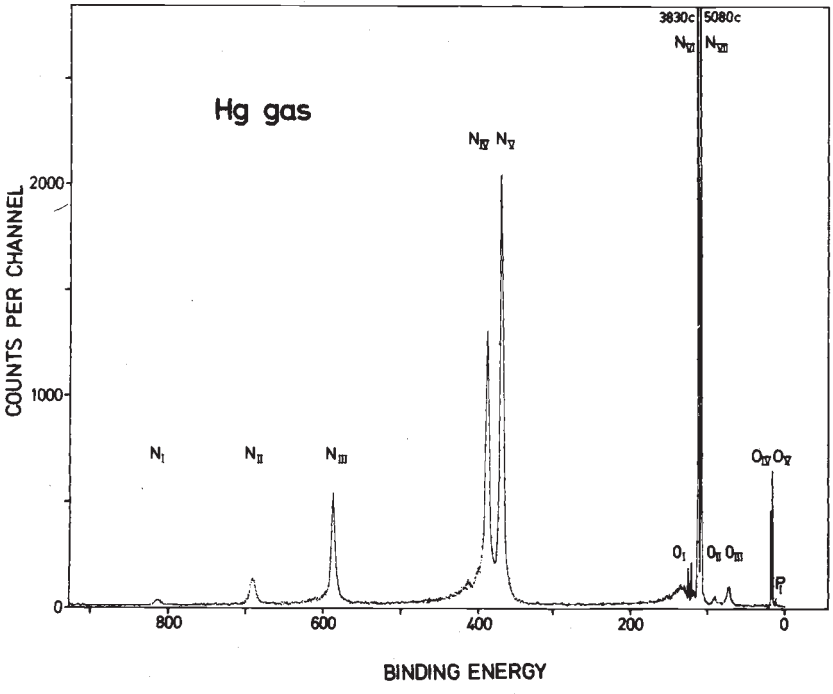

Fig. 6. ESCA spectrum of Hg vapour. Monochromatic AlK_α excitation.

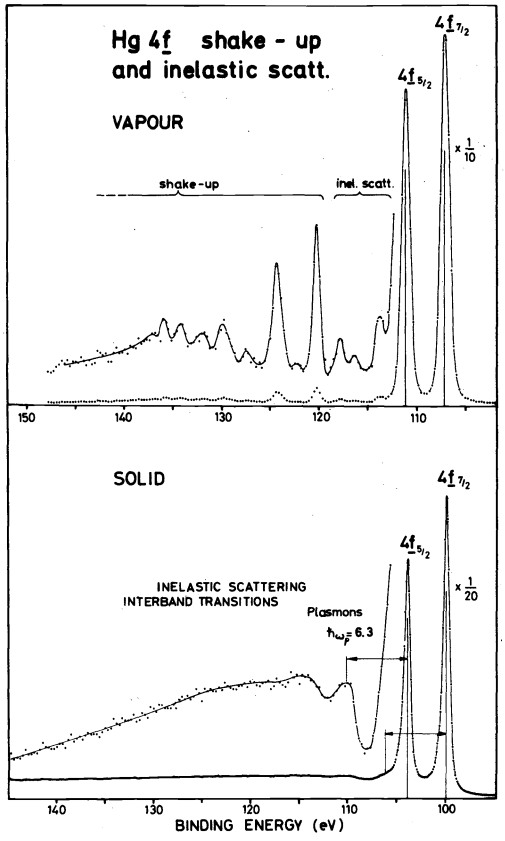

Fig. 7. ESCA satellite structures following the $N_{VI}N_{VII}$ main electron lines of Hg (see Fig. 6). Upper figure shows shakeup lines from gas phase, lower figure shows plasmon lines from solid phase.

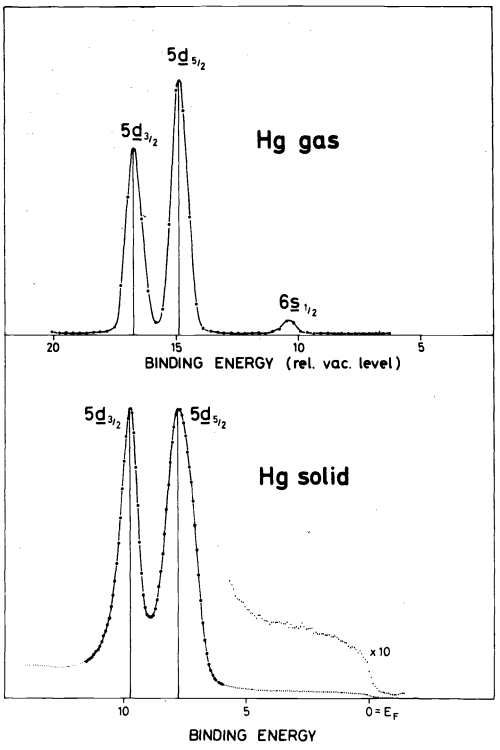

Fig. 8. The effect of condensation on electron lines close to zero binding energies. Upper spectrum from gas phase of Hg, lower spectrum the corresponding band structure for solid Hg.

one Mg atom in chlorophyll, one Co atom in vitamin B12 and the three disulfide bridges in insulin etc. ESCA shifts are related to the chemical bonding.

Figure 10 shows the electron spectrum from the 1s level of the carbon in ethyl trifluoroacetate. All four carbon atoms in this molecule are distinguished in the spectrum. The lines appear in the same order from left to right as do the corresponding carbon atoms in the structure shown in the figure. If the structure of the molecule is known, the charge distribution can be estimated in a simple way by using, for example, the electronegativity concept and assuming certain resonance structures. More sophisticated quantum-chemical treatments are preferably applied. Conversely, if by means of ESCA the approximate charge distribution is known, conclusions concerning the electronic structure of the molecule can be drawn.

Experimental evidence obtained so far for various elements in a large number of molecules indicates strong correlations between chemical shifts and calculated atomic charges. Such correlation curves can be obtained for many elements including sulfur, carbon, nitrogen, oxygen, phosphorus. Chemical shifts are also observed in the electron lines due to the Auger effect. Second-order chemical shifts from groups situated further away in the molecule (inductive effects) are also observed.

A further example of typical ESCA shifts (in acetone is given in Fig. 11. For comparison the spectrum observed when the AlK_α radiation was not monochromatized is inserted. One observes a substantial improvement of resolution and also decrease in signal: noise. The strongest

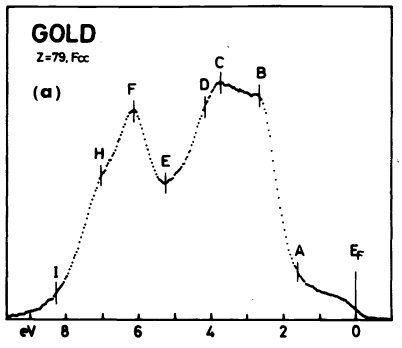

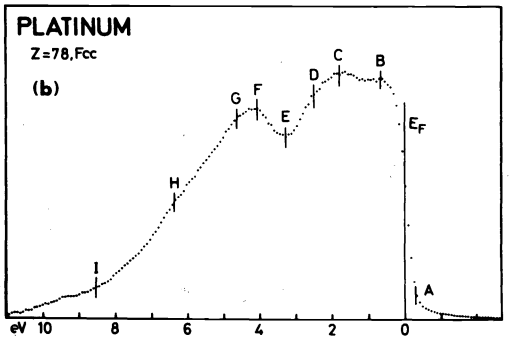

Fig. 9(a, b). Conduction electron band spectrum of gold (a) and platinum (b).

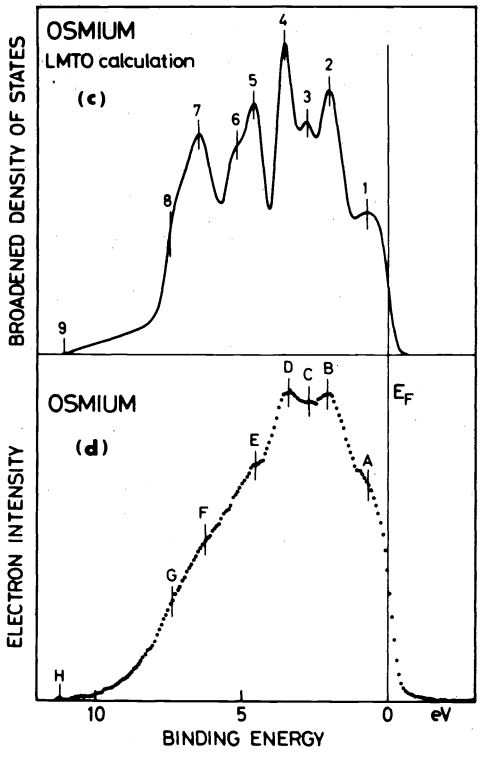

Fig. 9(c, d). Conduction electron band spectrum[2] of Os, theoretical (c) and experimental (d). The calculation of the density of states is based on a recent approach[3] called LMTO, 'linear combination of muffin tin orbitals'. The result is corrected for finite energy resolution but not for photocross-section dependence of band symmetry. The correspondence between the structures in the experimental spectrum (A, B, C . . .) and the calculated (1, 2, 3 . . .) is remarkably good.

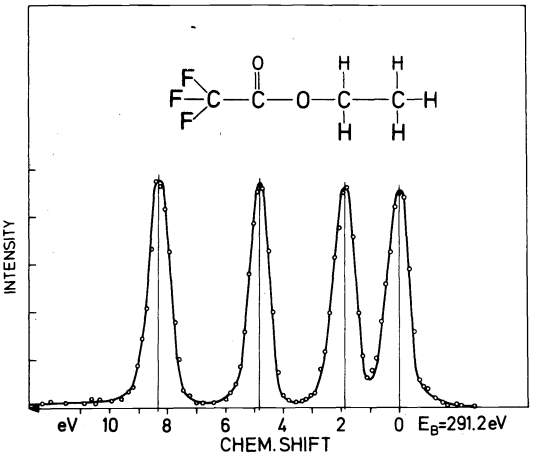

Fig. 10. The ESCA shifts of Cls in ethyl trifluoroacetate (monochromatized AlK_α).

C1s line belongs to the two equal carbons in the CH_3 groups, whereas the middle Cls line is the carbon in CO. The left Cls line is due to CO_2 which is mixed in as a calibration standard gas. This latter procedure has considerably improved the attainable accuracy (around 0.02 eV) in actually measuring the ESCA shifts and enables one also to get a consistent reference level for various gaseous compounds.

In a recent, not yet published study[4] of a number of benzene derivatives the above procedure has been used to investigate the ESCA shifts at various sites in the ring for different substituents. It turns out that one can obtain in this way some close correlations between ESCA shifts and chemical reactivity. First the unsubstituted benzene carbon is measured against CO_2 which is used as calibration for all the benzene derivatives. Figure 12 shows this

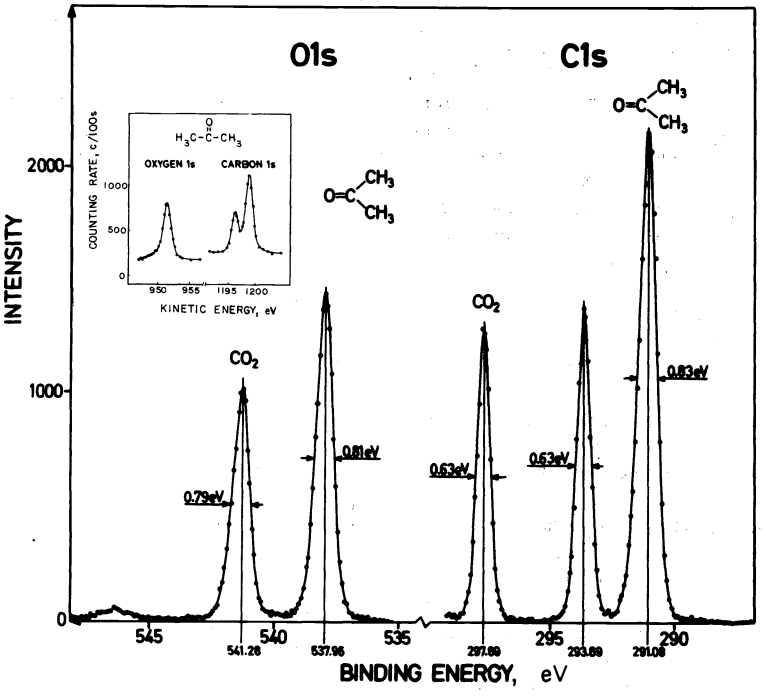

Fig. 11. ESCA shifts in acetone with carbon dioxide as calibration gas. Inserted in upper left part is a previous spectrum obtained without monochromatization of AlK_α.

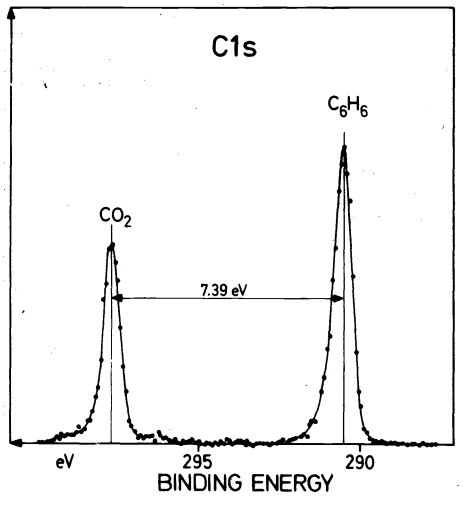

Fig. 12. C1s ESCA shifts between benzene and carbon dioxide.

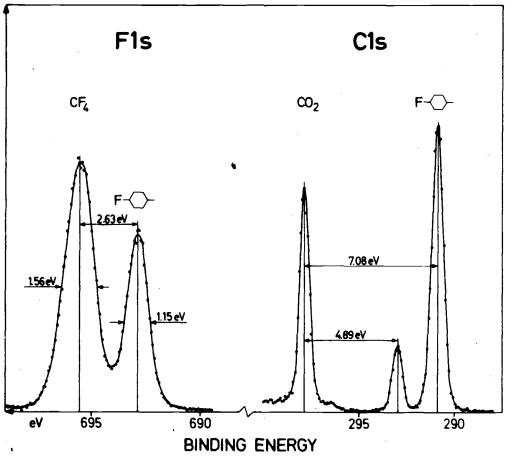

Fig. 13. ESCA shifts in fluorobenzene—referred to tetrafluoromethane (F1s) and carbon dioxide (C1s).

comparison. Figures 13 and 14 are given as representative spectra for two benzene compounds in the series of measured spectra. One can observe also that the ring carbons which are not directly situated at the substituent, also, exhibit ESCA shifts to various degrees. Some of the results are summarized in Figs. 15–17. In Figs. 15 and 16 the ESCA shifts, referred to Cls in CO_2, are measured at the starred carbon atom, whereas in Fig. 17 the ring carbon shifts, also referred to CO_2 are given.

It is interesting to correlate these shifts with chemical parameters such as Hammett's substituent constants (σ). A complete discussion is beyond the scope of this survey and the results are only indicated by the relation between measured ESCA shifts and the corresponding Hammett constants for the series of substituents as given in Fig. 18.

Molecules like O_2 or NO contain unpaired electrons and are therefore paramagnetic. Large classes of solid materials have similar properties. In such cases ESCA spectra show typical features called spin-, multiplet- or exchange splitting. The phenomenon was observed in oxygen when air was introduced into the source chamber of the ESCA

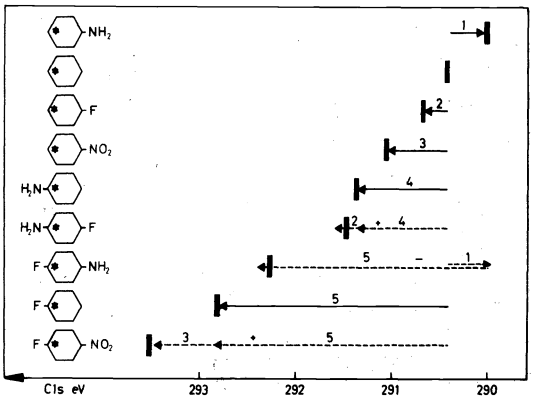

Fig. 15. C1s ESCA shifts in some benzene derivatives. This figure illustrates the range, ~3.5 eV, as well as the additivity of the substituent effects.

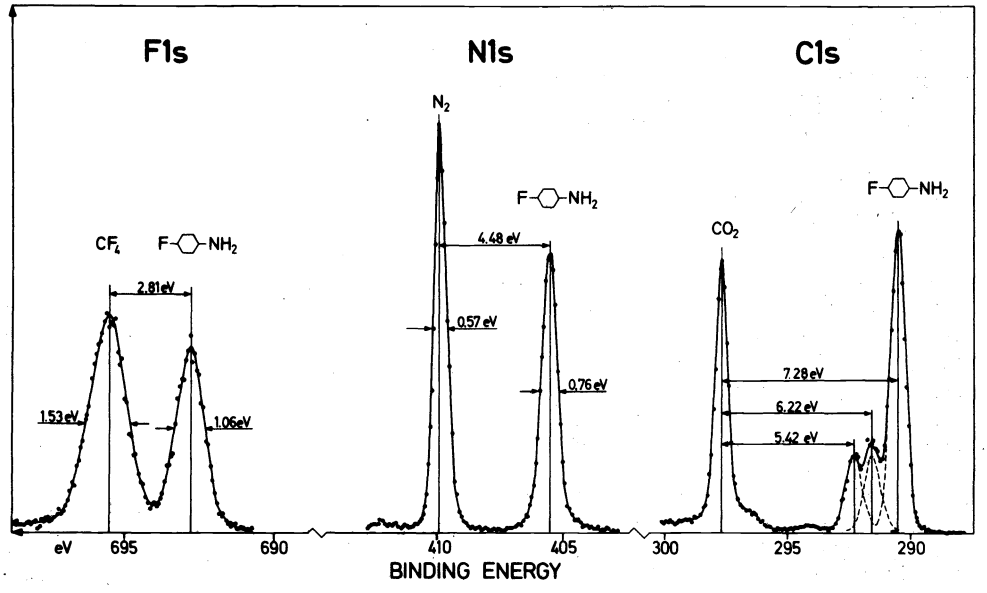

Fig. 14. ESCA shifts in parafluoroaminobenzene referred to tetrafluoromethane (F1s), nitrogen (N1s) and carbon dioxide (C1s).

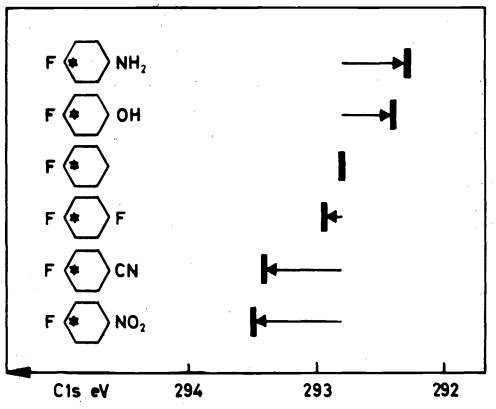

Fig. 16. C1s ESCA shifts illustrating the substituent effect in a series of para substituted fluorobenzenes. The shifts are due to the variation of one substituent in the same position and encompass a range of ~1.2 eV.

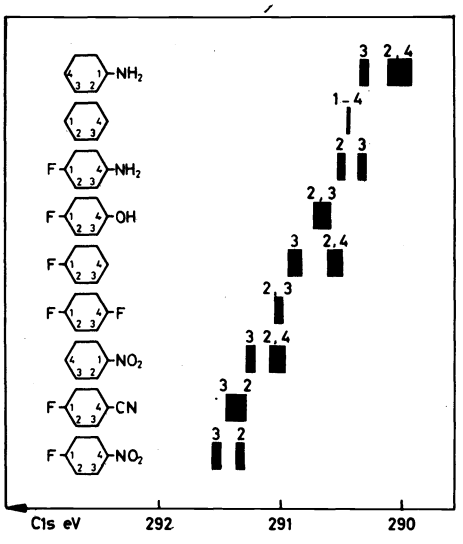

Fig. 17. Ring carbon shifts of the compounds shown in Figs. 15 and 16. The measured carbon atoms carry no substituents. The shifts are due to the 'relaying' of the primary substituent effect through the aromatic ring and encompass a range of ~1.5 eV.

instrument some years ago. The upper part of Fig. 19 shows the spectrum which was obtained when this phenomenon was first found and the lower part is the same spectrum as recorded with the new instrument with X-ray monochromatization. The 1s line of O_2 is split in the intensity ratio of 2:1. This spin splitting is due to the exchange interaction between the remaining 1s electron and the two unpaired electrons in the π_g-2p orbital, responsible for the paramagnetism of this gas. The resulting spin can be either 1/2 or 3/2. The corresponding electrostatic exchange energies can be calculated and correspond well with the measured splitting of 1.11 eV. Apart from oxygen and nitrogen, argon and CO_2 can be seen in spite of the low abundance of the latter gases in air. A statistical treatment of the data even exhibits the presence of neon (0.001%).

Recent improvements in resolution now enables one to measure the inherent widths of core levels in molecules.

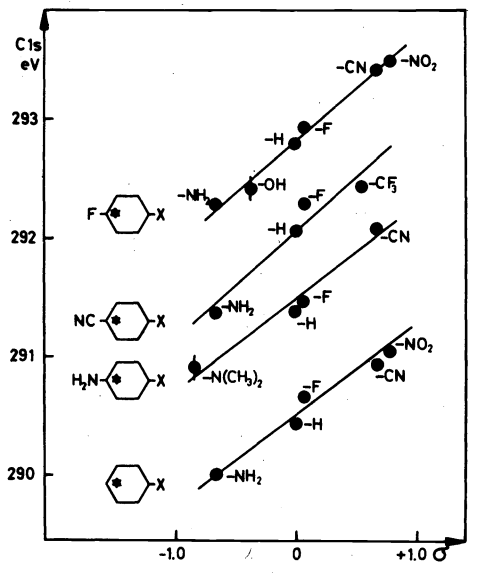

Fig. 18. C1s ESCA shifts in some para substituted benzene series versus Hammett substituent constants σ illustrating the correlation between ESCA shifts and reactivity parameters.

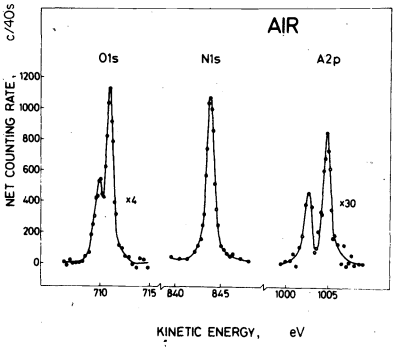

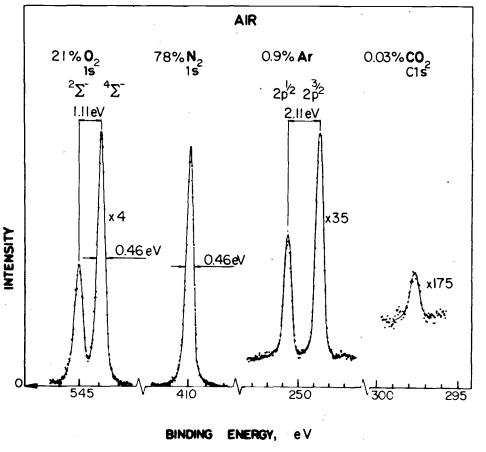

Fig. 19. Electron spectrum of air. The 01s is split into two components due to 'spin' or 'multiplet' splitting. Upper spectrum is the original one when this phenomenon was first observed. Excitation was performed by means of non-monochromatized MgKα radiation. Lower spectrum is taken more recently with monochromatized AlK$_\alpha$ ($\Delta h\nu = 0.2$ eV) using the prototype instrument (Fig. 5).

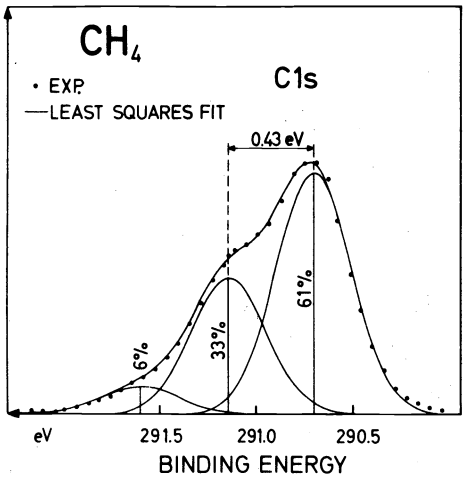

Fig. 20. C1s electron line of CH_4 showing vibrational structure.

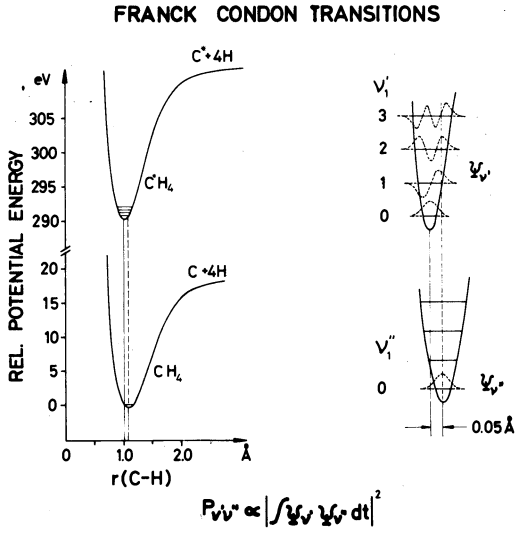

Fig. 21. Potential curves for CH_4 and CH_4^+ explaining vibrational structure at photoionization of the carbon core level.

As an example, Fig. 20 shows the line profile of the Cls in CH_4. It turns out that this line can be separated into three components caused by the symmetric vibration when photoionization occurs in the 1s level of the central carbon atom. Figure 21 demonstrates what happens. When the electron leaves the carbon atom the latter shrinks about 0.05 A. The minimum of the new potential curve for the ion will consequently be displaced by the corresponding amount and Franck–Condon transitions which take place will then give rise to the observed vibrational fine structure of the electron line and with the intensities given by the Franck–Condon factors quoted in the figure. This finding can be correlated with a series of recent observations (Ref. 1, p. 70) in our laboratory, that there exist vibrational fine structures in X-ray emission lines. Combined, these results show that vibrations occur in these molecules during X-ray emission both in the initial and the final states.

There are also other causes of line broadenings in molecules and solids which can now be studied quantitatively by means of electron spectroscopy. Two spectra may illustrate more generally what one observes concerning linewidths in the case of solids, namely NaCl (Fig. 22) and Cu (Fig. 23). In these spectra all levels with their inherent widths are recorded, from binding energies 1400 eV to the valence and conduction band at zero binding energy. In the case of NaCl, being an ionic crystal, the ionicity can be measured simply by taking the distance between the loosest bound levels in the valence

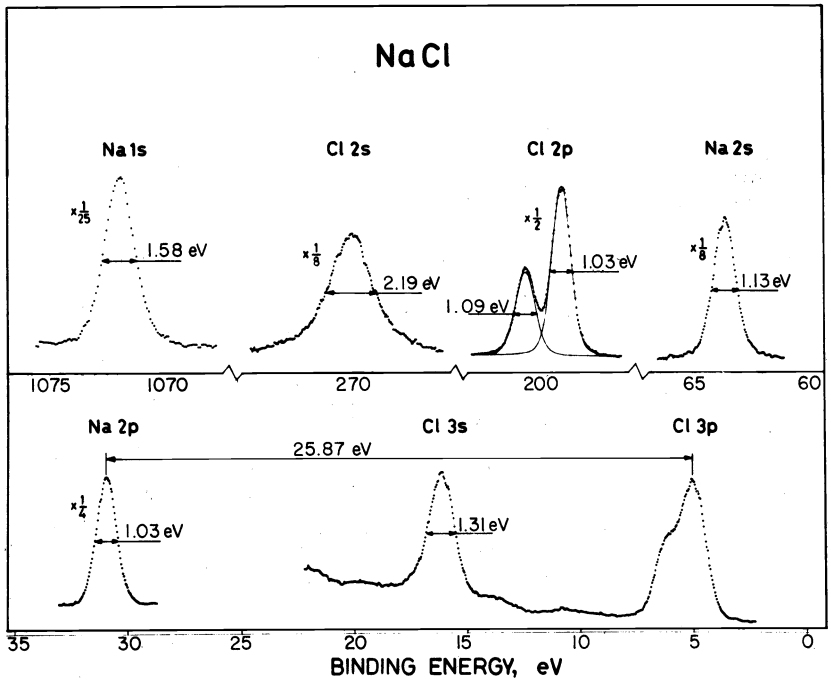

Fig. 22. Electron spectrum of NaCl showing the core and valence electron lines with their inherent widths. There is a partial splitting of the C1 3p level due to a lattice effect.

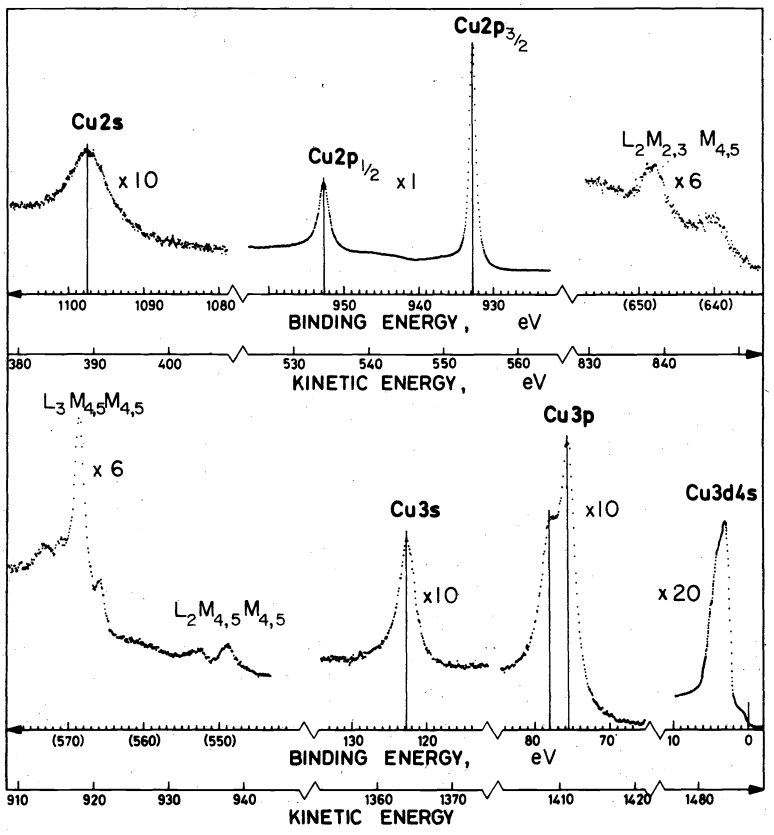

Fig. 23. Electron spectrum of Cu showing the core lines with their inherent widths and also the conduction band. See also the more detailed shape of the band given in Fig. 24.

region of the electron of the cation, Na2p, and anion, Cl3p.

It was mentioned before that conduction bands can be studied for metals and their alloys. Figure 24 shows a recording of pure copper (upper spectrum), pure palladium (middle spectrum) and the alloy CuPd (60% Cu and 40% Pd, f.c.c.). There are many interesting features in these spectra. First, one observes in the case of Cu a symmetric core line ($2p_{3/2}$) and a conduction band, having a low density of states at the Fermi edge. For Pd the contrary is seen, namely quite asymmetric core lines ($3d_{5/2,3/2}$) and a high density of states at the Fermi edge of the conduction band. When these metals alloy there is a remarkable decrease in both linewidth and also asymmetry of the Pd core lines and the slope at the Fermi edge is less steep which means that the density of states is decreased compared to pure Pd. There are also changes in binding energies of the core levels. The asymmetry of core lines for metals is connected with the density of states as observed in the conduction bands in the ESCA spectra. Asymmetries of core lines for various metals having high density of states at the Fermi edges are shown in Fig. 25. It is likely that the core electrons loose more easily a small part of their energies to create electron-positive hole pairs when there is a high density of states in the conduction band at the Fermi edge. These electrons are responsible for the electronic specific heat. If the asymmetry of core lines is plotted as a function of this quantity for the metals studied in the previous figure one obtains the relation shown in Fig. 26. These problems should be further studied and any connection between these properties and catalytic effects (see below under Surface Sensitivity) exhibited by some of these metals more closely investigated. The effect of alloying on these results also needs investigations.

YMζ AND UV EXCITED ELECTRON SPECTRA

So far we have been dealing with (monochromatized) X-ray (AlK_α) excitation of electron spectra. This is probably the excitation mode leading to the widest diversity in applicability, since core levels and their shifts, apart from the valence levels, are accessible this way. There are also some theoretical reasons why the electron spectra are easier to interpret when the excitation energy is high enough to expel the electrons far away from empty molecular states. The synchrotron radiation provides a great flexibility in this respect but due to many obvious reasons it has limitations in its practical applicability.

Before giving some examples of UV excited spectra it is appropriate to discuss a complement to the AlK_α mode of X-ray excitation. Some years ago it was suggested that ultrasoft X-rays from ZrMζ or YMζ, energies of 151.4 eV and 132.3 eV, respectively, be used for this purpose.[5] There are some technical difficulties due to the extremely high absorption rate of these soft X-radiations both in any small surface contamination of the anode itself and in the window to be used. However, good progress has recently been made by several groups[6-8] and in Fig. 27 one example of a spectrum is shown, as obtained in laboratory.[8] In this experiment a water cooled, rotating yttrium anode was used with a positive potential with respect to the source chamber window, a very thin carbon foil (20 $\mu g/cm^2$). Electrons, scattered from the anode, are retarded to zero energy before reaching this

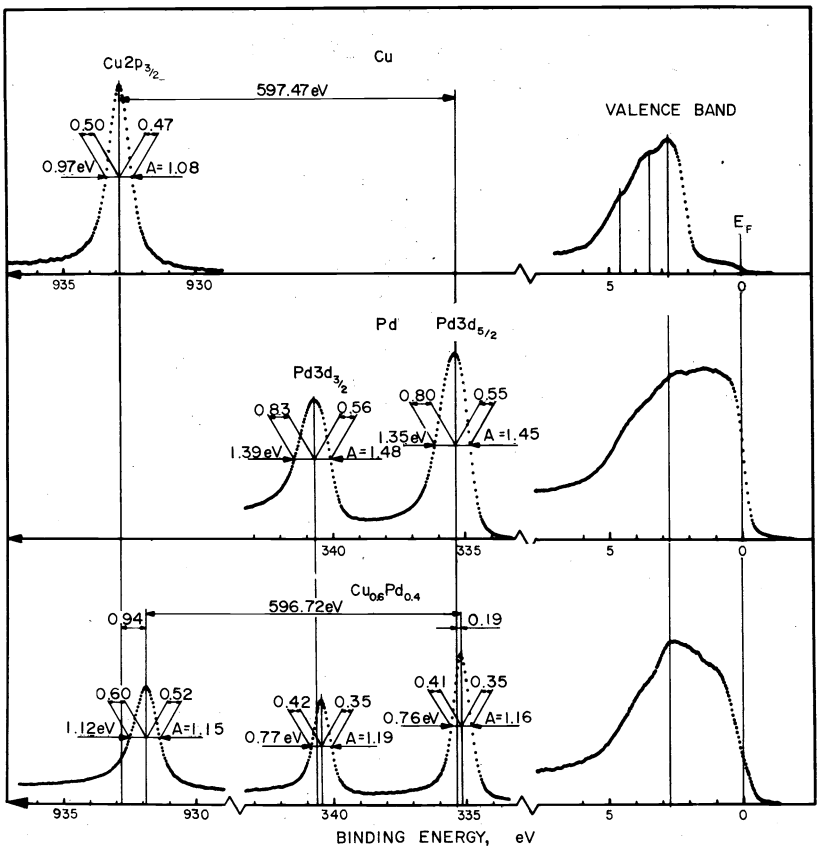

Fig. 24. Conduction bands of Cu and Pd and the alloy CuPd (60% Cu and 40% Pd, f.c.c.). The asymmetric line shapes of the Pd core lines are strongly influenced by the alloying with Cu × 30 and are related to the changed slope at the Fermi edge of the alloy.

foil. To keep the yttrium anode constantly clean, there is an oven situated below the rotating anode, which continuously evaporates fresh yttrium metal onto the anode surface. These arrangements turn out to provide the necessary conditions to enable one to run yttrium Mζ excited electron spectra for long periods of time at a constant X-ray level. A multidetector system in the focal plane of the ESCA instrument ensures a high speed of accumulating the data. The spectrum given in Fig. 27 shows the valence region of N_2. In the upper part the N_2 spectrum excited with monochromatic AlK_α is given, in the lower part with YMζ. Inserted is a more detailed study of the three valence orbitals which show line-broadenings due to vibrational structure. The width of each line is set by the inherent width of YMζ, around 0.6 eV. Below the spectrum is indicated the spectrum which is obtained by UV-excitation using HeI radiation at 21.22 eV. The most interesting feature of this comparison of electron spectra performed at different excitation energies is the widely different relative intensities of the electron lines in the three modes. This is due to the dependence of the photoelectric cross-section on not only the energy of the exciting radiation but also on the symmetry of the molecular level concerned. Consequently, from comparisons of this kind orbital symmetry assignments can be made experimentally, provided the cross-sections are determined either theoretically[9] or semi-empirically from a number of known cases. The so-called intensity model (Ref. 1, p. 70) based on the MO-LCAO approximation has been used extensively in ESCA during recent years to treat these problems.

In our laboratory another possibility, i.e. using a polarized He light source, is being studied. In this case the relative intensities of the valence electron lines are recorded as a function of the angle between the electric vector of the photons and the emitted photoelectrons. Due to the losses at the successive reflections of the UV light at the mirrors (these have to be flat to within 50 Å) at present to get polarized light required a substantial reduction in intensity is inevitable and has to be compensated for by a high efficiency in the rest of the system.

Three examples of UV excited spectra are given in Figs. 28–30, showing the valence electron spectra of water vapour[10] (Fig. 28), benzene [11] (Fig. 29) and three metal hexafluorides[11] (Fig. 30), namely MoF_6, WF_6 and UF_6. In Fig. 28 the vibrational structure of the electron bands corresponding to the $1b_1$ and $2a_1$ valence orbitals are well resolved. For the $^2A_1$ state a vibrational progression of the ν_2 bending mode consists of 20 members. The difference between H_2O and D_2O is also striking. A careful study of the $H_2{}^{16}O$ and $H_2{}^{18}O$ spectra reveals an isotopic effect also in this case. Vibrational structures are present in both the benzene and the hexafluoride spectra but due to the increased complexities introduced by more degrees of freedom for vibrating modes the various vibrations are not always possible to resolve. Where they can be resolved a high precision in the ionization energies is always possible to attain, due to the extremely

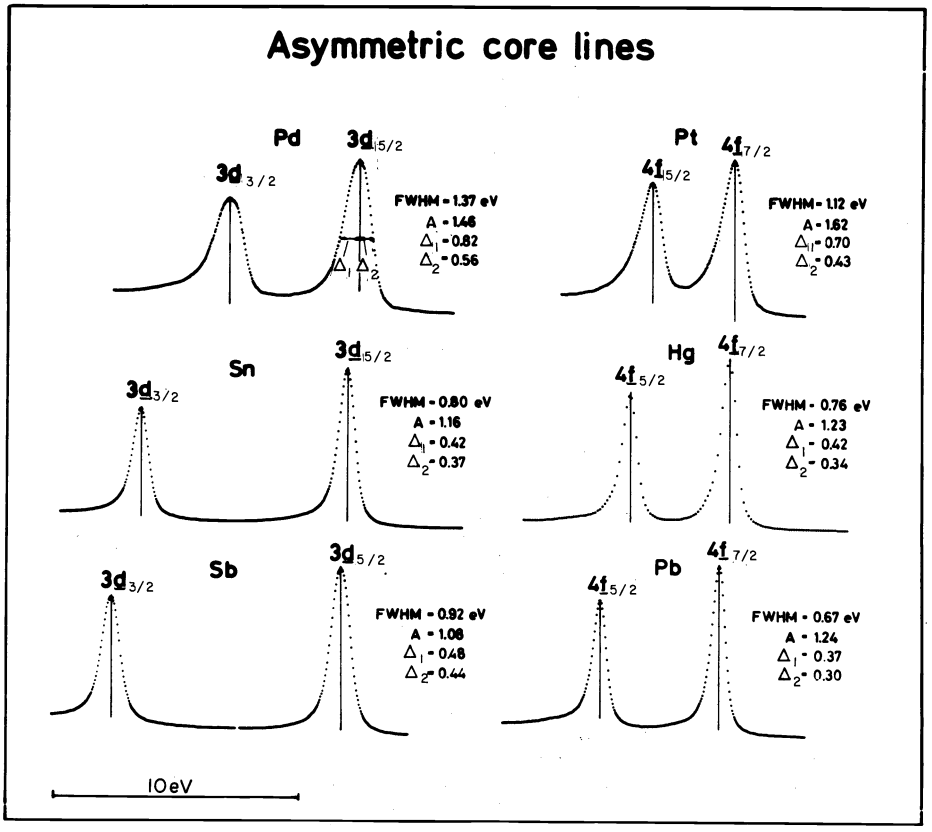

Fig. 25. Asymmetries of core lines of various metals having high density of states at the Fermi edges of their conduction bands.

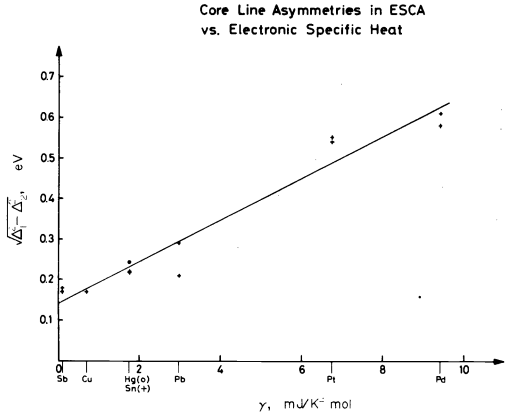

Fig. 26. Asymmetry of core lines (see Fig. 25) as a function of the electronic specific heat of the metals.

narrow HeI resonance line at 21.22 eV. Electron linewidths around 10 meV can be obtained with an accuracy in the line positions of 1 meV.

SURFACE SENSITIVITY

The analytical sensitivity of ESCA is related to its property of being a surface spectroscopy. The depth of information, which is the electron escape depth without any energy losses, is limited to < 50 Å, depending somewhat on the material and, in particular, on the energy of the electrons being emitted. The electron escape depth as a function of electron energy is a parabola-like function with a minimum at about 100 eV, where the escape depth is some 3 Å.

We have seen that bulk properties such as conduction bands are reproduced in the ESCA spectra and many other examples could be given which show that the analysis of the materials usually corresponds to the composition and properties of the matter in bulk. One further example of some practical interest is given in Fig. 31, showing the C1s electron spectrum of a plastic material, namely Viton with two different compositions, Viton 65 and Viton 80. The branching and relative compositions of these two polymers are well reproduced in their ESCA spectra.

The surface sensitivity is, however, likely to be of special importance for the application of ESCA. In particular if the emitted electrons are being looked upon at a small angle relative to the surface by the electron analyzer, the escape depth may correspond to only one single molecular layer, and within this layer, which is by definition truly a surface layer, the composition and chemical bondings can in principle be analyzed by ESCA. Adsorption of gas molecules onto a surface, corrosion, heterogeneous catalysis, depth diffusion, and surface reactions are natural research objects. Such studies are known to be difficult to perform, no matter what technique is being used and require clean surfaces (often ultrahigh vacuum) and well defined and controlled experimental conditions. One of the main roads of developments in electron spectroscopy is to explore these possibilities. Already interesting information is being obtained from studies in this promising field. To take a few examples,[12] it is possible to distinguish between CO standing up (α form) with either the O or the C atom on the W

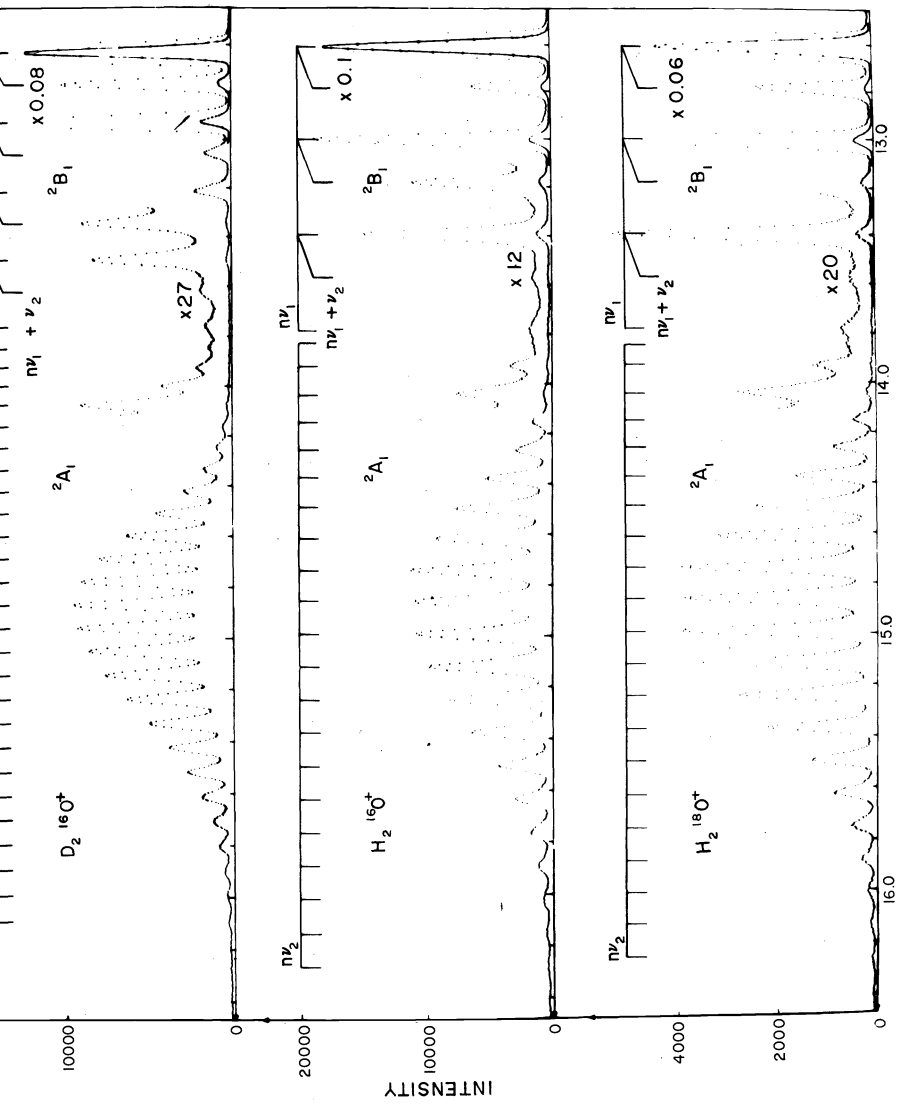

Fig. 28. Part of the valence electron spectrum of H_2O excited at $h\nu = 21.22$ eV (HeI). One observes isotope effects between $D_2{}^{16}O$, $H_2{}^{16}O$ and $H_2{}^{18}O$. The $^2A_1$ state has a vibrational progression of the ν_2 bending mode which consists of 20 members in the electron spectrum.

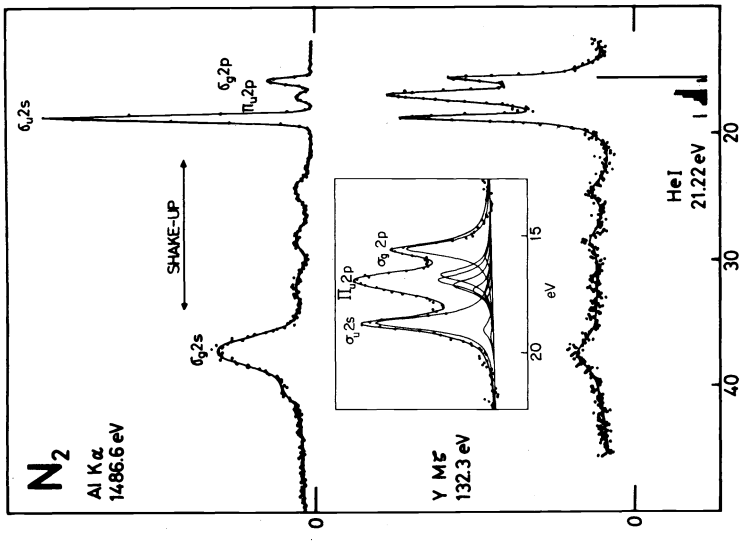

Fig. 27. Valence electron spectra of N_2 obtained by monochromatized AlKα excitation (upper spectrum) and by YMζ excitation (lower spectrum). The three main lines are plotted in more detail and deconvoluted to indicate inherent electron linewidths (0.6 eV) and vibrational structures. Indicated at the bottom of the figure is also the HeI-excited valence electron spectrum. Observe the widely different intensity ratios in the three cases.

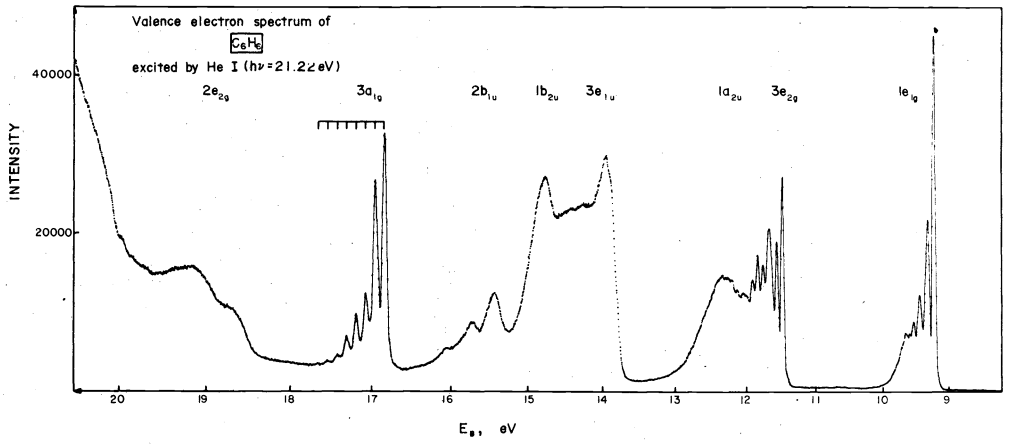

Fig. 29. The valence electron spectrum of benzene, excited at $h\nu = 21.22$ eV.

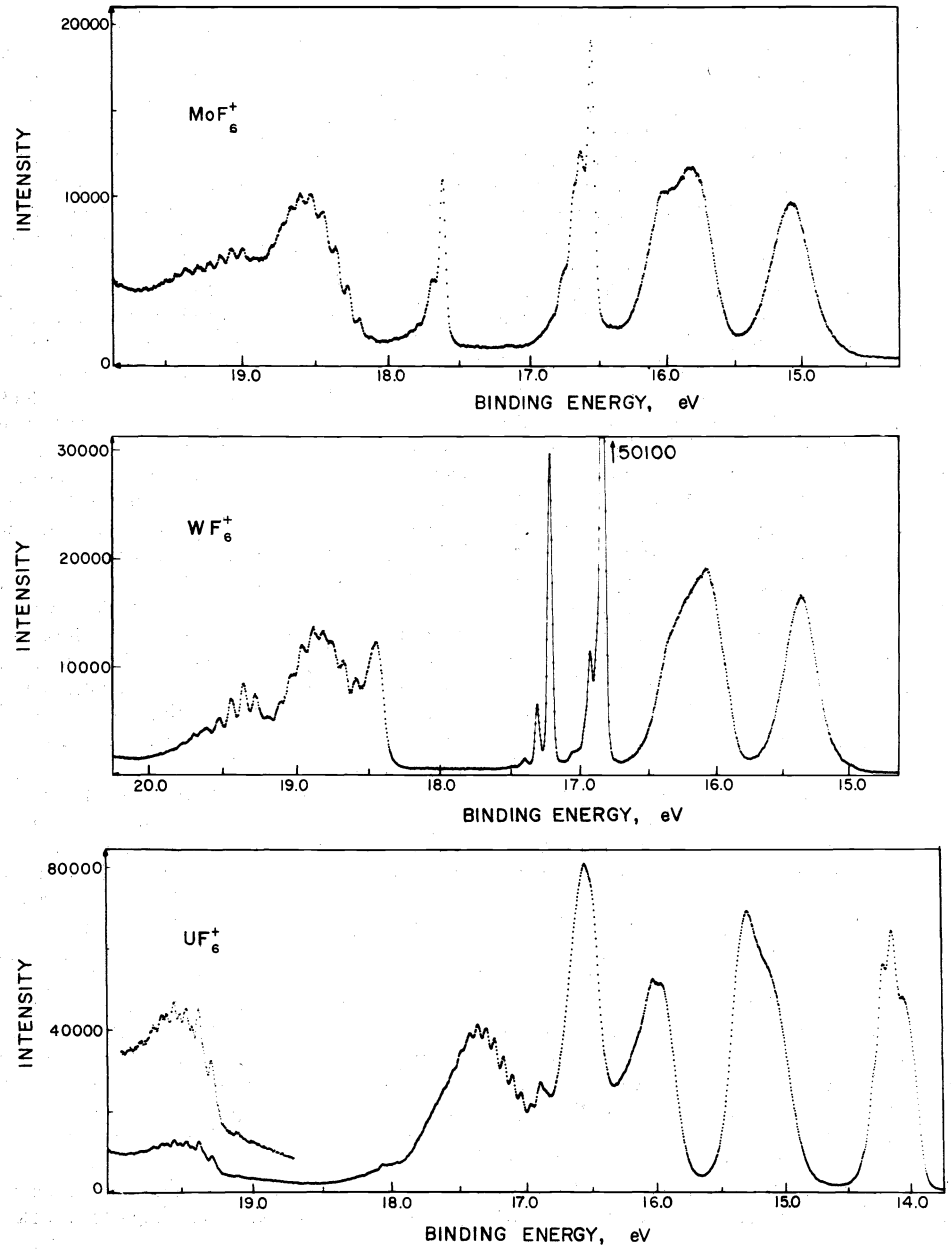

Fig. 30. The valence electron spectra of MoF_6, WF_6 and UF_6, excited at $h\nu = 21.22$ eV.

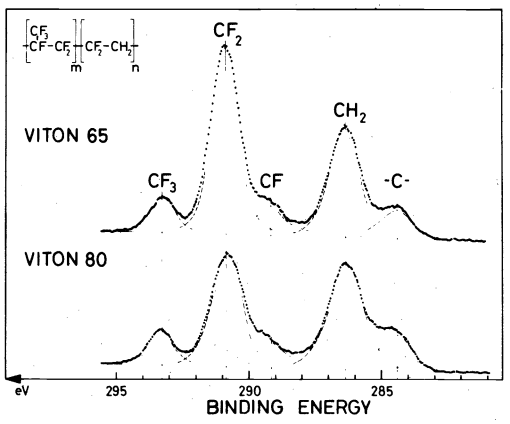

Fig. 31. ESCA spectra of Viton 65 and Viton 80 polymers.

surface or CO lying down (β form). In the β form CO seems to be dissociated on the surface of Mo. These conclusions can be drawn from the differences in ESCA chemical shifts between the free CO molecule and when CO is adsorbed on the surface, and is due to the metal surface ability to supply electrons to polarize the electron hole left behind during photoionization. This influences the "external" relaxation energy and decreases the binding energy as observed in ESCA. These are typical "final state" effects, just as are shake-up electron lines or vibrational line structures. It is also likely[12] that heterogeneous catalysis is dependent on final state effects when in the extreme case an electron is transferred from one molecule to another to form an activated complex. Such a transfer is facilitated when conduction electrons from the catalyzer metal can shield the resulting electron hole. This will decrease the binding energies of the electrons and reduce the potential barrier leading to the final reaction products, since an additional source for external relaxation is provided.

There are also "initial state" effects which are influenced by surface conditions. For example, molecules lying on a surface, say benzene, expose their π-orbitals more strongly than the σ-orbitals and are consequently more influenced by the surface. This results in an increased π-orbital binding energy. The best surface sensitivities reported with present days technique so far is $2 \cdot 10^{-3}$ atomic layer for a heavy metal evaporated onto a surface.[13]

It has been suggested and also tried to combine the surface sensitivity of ESCA with a scavenge technique to extract various ions in very low concentrations from a solution onto a fibreglass surface, which has organic functional groups attached to it. In this first trial, Hercules[14] in this way reached sensitivities for lead, thallium and mercury in solutions as high as 5 ppb. Quite recently[15] this figure has been further improved to ~0.1 ppb.

AUGER ELECTRON SPECTRA

Photoionization, giving rise to photoelectron spectra, always accompanied by Auger electron emission and whether the excitation is caused by monochromatic X-radiation or by a beam of electrons the Auger electron spectra characteristic for that molecule will be recorded in an ESCA instrument. The emission of the Auger electron lines is due to transitions between an initial state having one core electron vacancy and a final state having two vacancies. The energies of the Auger electron lines are independent of the energy and the kind of exciting radiation. These lines provide information about the molecular structure which is complementary to the photoelectron lines. For example, Auger electron lines are similarly subject to chemical shifts. Auger electron spectra are complicated to interpret for the light elements belonging to the first row (C, N, O etc.) since the valence orbitals are involved in the transitions.[16,17] From the next row elements, starting with Na, Mg, Al, Si, P, S, and Cl, however, KLL Auger transitions occur between core levels and give rise to a characteristic group of lines with one line dominating the other ones in intensity, namely the one which can be described as the $KL_{II}L_{III}$ transition ($2s^2 2p^4 ({}^1D_2)$).

Figure 32 shows this Auger electron line group for Mg and MgO and at an intermediate stage of oxidation. For the metal one can also observe series of volume plasmon lines accompanying primary Auger lines as satellites. The Auger chemical shift between Mg and MgO amounts to 5.2 eV which largely surpasses the chemical shift between the photoelectron lines, being 1.1 eV.

In order to study more closely the relationships between Auger- and photoelectron line chemical shifts for free molecules and for solids in a systematic way, an arrangement has been designed which is shown in Fig. 33. The external coil of a magnetic ESCA instrument has been removed in the photo to show the sample housing with the various excitation facilities incorporated in this apparatus. In order to get high Auger electron line intensities an electron gun with quadrupole focussing lenses etc. is attached to the bottom of the housing, the electron beam being directed upwards and hitting the gas sample volume (or the solid sample) through a small hole in the bottom of this chamber. The sample chamber is introduced and interchanged from above through a vacuum lock device. X-ray excitation can simultaneously be done by means of the strong electron gun inserted into the back wall of the housing and the watercooled rotating anode at the other side wall. A He lamp can, furthermore be introduced from above. There is a two stage differential pumping system around the source chamber to enable the study of gaseous samples. The Auger and photoelectrons leave the source chamber through a narrow slit and pass a small four-component electrostatic lens system forming an image at the entrance slit to the analyzer, after being retarded to a low energy in order to increase the energy resolution. At the other side of the double focussing analyzer, i.e. after 255°, there is a multidetector system along the focal plane of this magnetic ESCA instrument.

The first series of studies concern Auger electron spectra of various sulfur compounds as compared to the corresponding photoelectron spectra. Recent theoretical work by means of so-called "transition potentials" shows that the Auger electron spectra[18] for molecules can be quantitatively evaluated this way. Previous calculations by this method on binding energy shifts at photoionization (ESCA shifts)[19,20] showed that this approach gave results in very good agreement with experiment.

By changing continuously the electron gun voltage and keeping the analyzer keeping the Auger line in focus, "excitation yield" spectra can be done by means of the new arrangement. These "spectra" are interesting to follow around and above the threshold for the Auger process. The arrangement also allows, in principle, some other experiments to be done, such as pulsed double beam excitation which may concern excited and fragmented molecules etc. Microwave or UV laser pulse techniques are also of interest in this context.

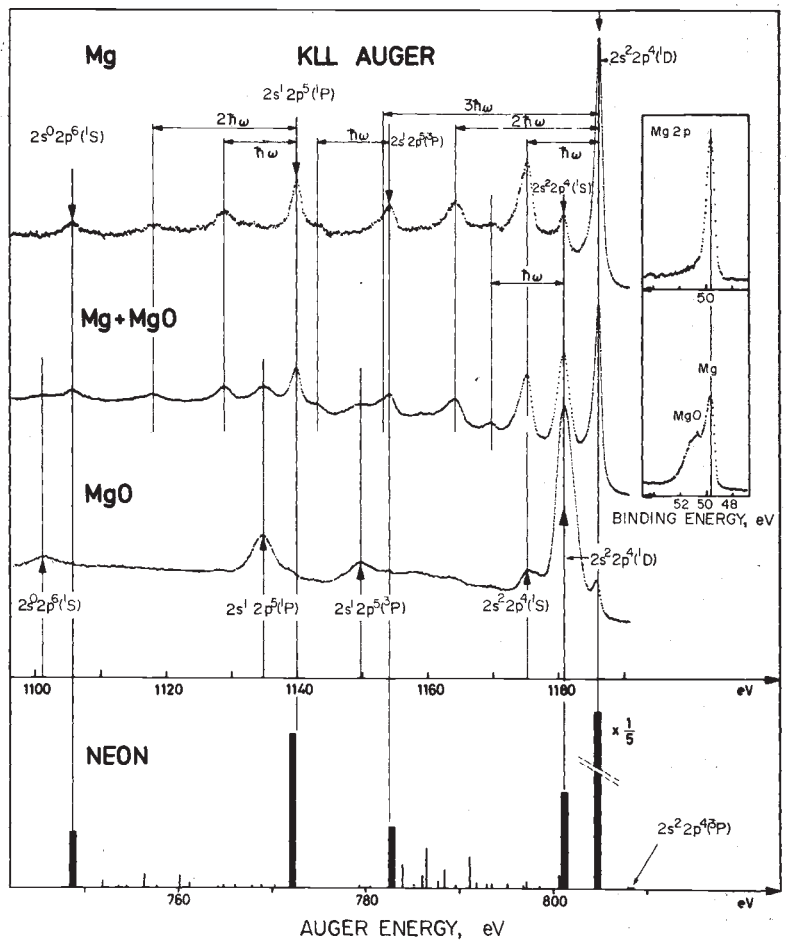

Fig. 32. Mg KLL Auger electron spectra at different stages of oxidation as obtained in ESCA. Upper spectrum is from a clean metal surface, lower spectrum from the oxidized metal (with only a trace of metal) and the middle spectrum is from an intermediate oxidation. Volume plasmon lines are observed. For comparison, the positions of the Ne KLL Auger electron lines are given below, as recorded in the ESCA instrument by means of electron beam excitation.

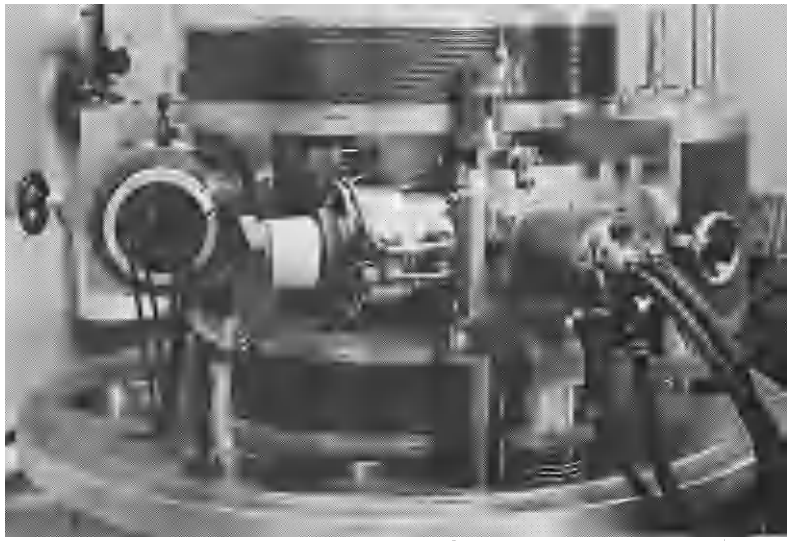

Fig. 33. New arrangement for simultaneous Auger and photoelectron line chemical shift measurements for gases and solids in a magnetic ESCA instrument. Excitation can be made by an electron beam (from below), X-rays (from the side) and UV (from above). The sample chamber is introduced from above through the vacuum lock device. Excitation can also be performed by pulse techniques.

ESCA SPECTRA OF LIQUIDS

So far we have discussed electron spectra of several kinds of gases and solids. During the last two years we have been trying to extend the ESCA techniques to include also liquids. Our first arrangement consisted in forming a "liquid beam" of the sample inside the source compartment of the ESCA instrument. Figure 34 shows this arrangement. The liquid or solution to be studied is continuously circulated by means of a pump. The liquid is pumped either up into the nozzle ($\phi \sim 0.7$ mm) which then forms the beam or through a by-pass tube back into the reservoir. Valves can be adjusted to control the speed of the liquid beam through the nozzle. The nozzle can be slid on the top of the source housing in order to allow a precise adjustment of the liquid beam in front of the entrance slit of the analyzer of the ESCA instrument. When an electron spectrum from a liquid is recorded one can, in general, obtain a signal from the vapour as well as from the liquid itself. We found that we could actually separate the two spectra by adjusting the beam position relative to the slit (shown in Fig. 35). The liquid to be studied was formamide ($HOCNH_2$). When the beam is to the left of the slit only the C1s line from the vapour is recorded. When the beam is gradually moved in front of the slit a line from the liquid itself grows up at a distance of 1.6 eV from the gas line. At a certain position of the beam the gas line is completely suppressed and only the liquid line is recorded. A further movement of the beam restores the gas line. The reason for this fortunate behaviour is the shadowing effect of the liquid beam itself on the vapour which is excited by the X-rays in this geometry.

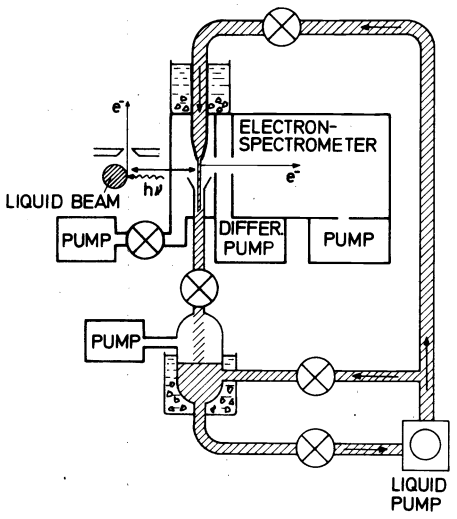

Fig. 34. First arrangement to form a 'liquid beam' in ESCA.

Figure 36 is a recording of the O1s, N1s and C1s from $HOCNH_2$ at a beam position which allows both the liquid and the gas to be recorded simultaneously. A very small trace of water in the liquid produces an O1s line (to the left) in the gas phase.

Figure 37 is a liquid spectrum of a solution of a salt, namely KI in formamide. One observes the ESCA lines from both iodine and potassium.

Since these experiments were completed we found a

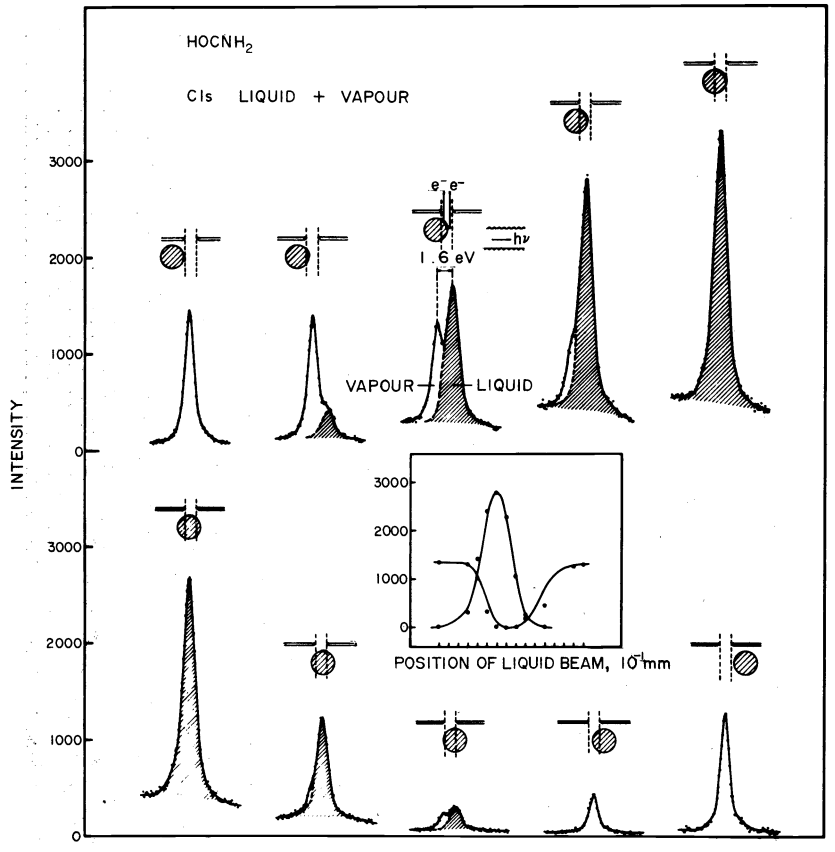

Fig. 35. ESCA lines from the gas phase and the liquid phase as a function of liquid beam position relative to the analyzer slit.

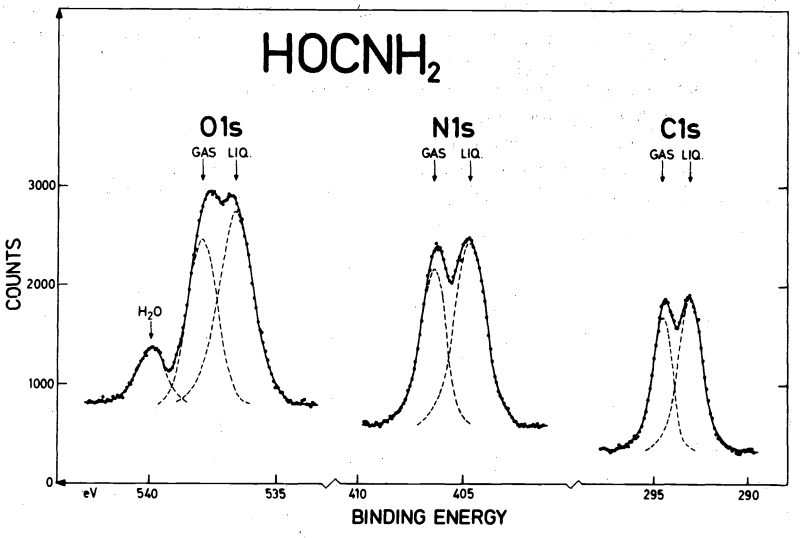

Fig. 36. Electron spectrum of formamide in beam position to yield both gas and liquid lines.

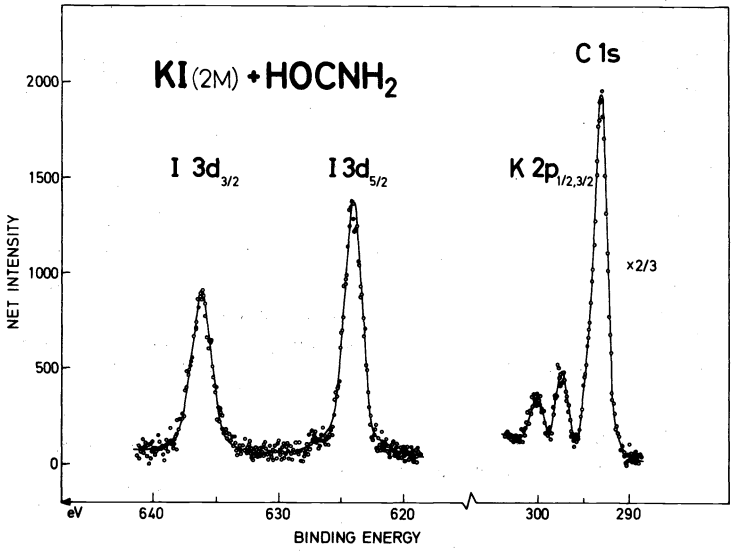

Fig. 37. Spectrum of a dissolved salt, KI, in formamide.

somewhat better method[21] of arranging liquid studies. This arrangement (see Fig. 38) consists of a thin stainless steel wire running from one bobbin to another. The wire passes down into a small beaker of liquid and then, after being covered with a thin skin of the liquid, it proceeds upwards along and in front of the slit of the ESCA analyzer. The wire at the same time provides a stabilization of the electric potential of the liquid. This system can run for some hours without recharging and works quite satisfactorily. Many core and valence electron spectra for liquids and also Auger electron spectra from dissolved salts have now been recorded with this system.

Figure 39 shows the electron spectrum from glycol $(CH_2(OH))_2$. The left spectrum is from the liquid. The extra C1s peak with the upper part of the figure has no correspondence at the O1s line and disappears in fact after the wire has cleaned the liquid surface from carbon contaminants at a higher speed (see figure below). The right figure shows the spectrum when the wire is adjusted for recording both liquid and gas phase (above) and only gas(below).

Figure 40 shows[22] the valence electron spectrum of formamide for the liquid and gas phases separately. A characteristic change of the orbitals at condensation can be explained in terms of intermolecular interactions in the liquid. The liquid spectrum is consistent with hydrogen-bonded linear chains of molecules in the liquid. Also mixtures of liquids can be studied.[23]

Finally, Fig. 41 shows the first Auger electron spectrum from a liquid, namely from sodium when $Na_2(CN)_2$ is dissolved in $(CH_2OH)_2$.

PRESENT DEVELOPMENTS

The field of electron spectroscopy is now a well established field of research with numerous applications and with many possible ways to proceed, some of which have been indicated in this survey. Already with present days' techniques one can explore large fields and add much new

information about the electronic structure of molecules and condensed matter. With further improvements this spectroscopy is inherently capable of developing in several directions, one of the most interesting ones being surface science. Ultrahigh vacuum technology and improved sample handling are necessary prerequisities for progress along these lines. Higher intensities and better resolution can also soon be expected. This means increased sensitivity and should normally result in a better chance of study phenomena which may now be at the borderline to the feasible. One could list many examples of this kind, among them time studies of surface reactions etc. In all cases,

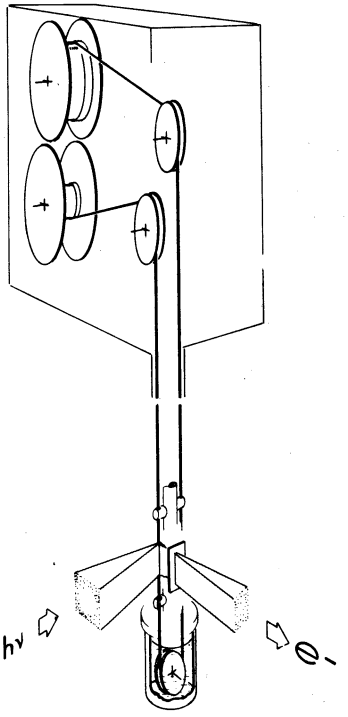

Fig. 38. Wire system for ESCA liquid studies.

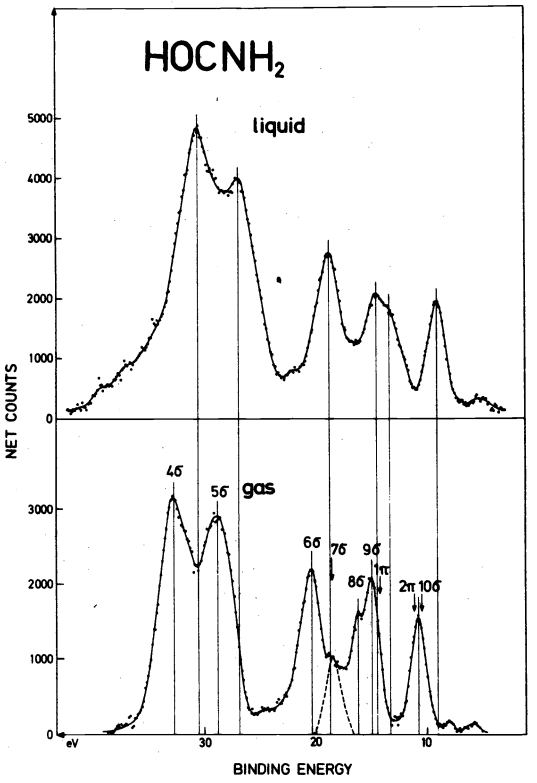

Fig. 40. Valence electron spectrum of formamide for the liquid and gas. At condensation hydrogen bonded linear chains of molecules in the liquid are formed.

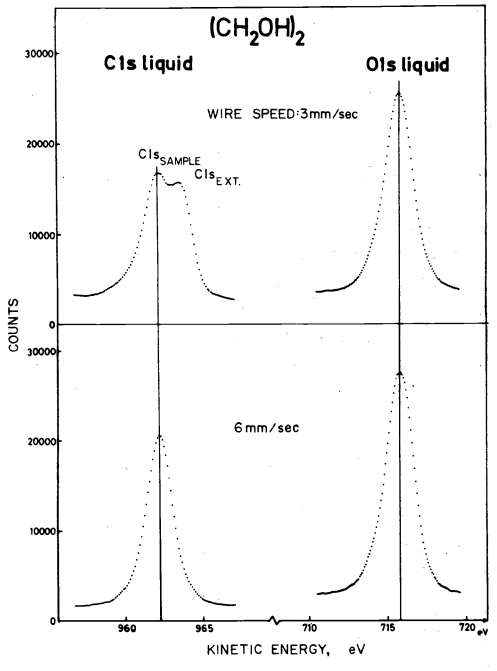

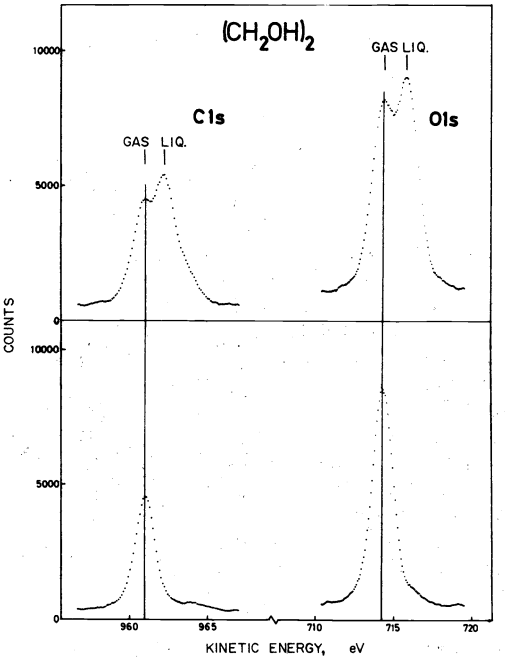

Fig. 39. Electron spectrum from glycol using the wire system shown in Fig. 38. Left figure: liquid with extra line due to carbon impurity at the surface (upper part) and after wire has cleaned surface at higher speed (lower part). Right figure: wire adjusted for recording both liquid and gas phase spectra.

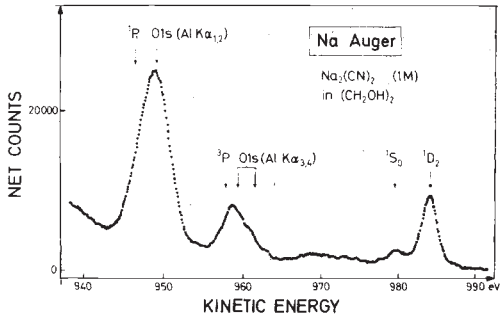

Fig. 41. First Auger electron spectrum from a liquid. One observes the main KLL Auger lines from sodium in $Na_2(CN)_2$ dissolved in glycol. Also the 01s core line from glycol is recorded.

however, increased intensities mean more convenient conditions to study phenomena which require the accumulation of large amounts of data. As an example, we observed some hears ago in our ESCA instrument a kind of "internal" electron diffraction[24] occurring during an ESCA process in a crystal. A NaCl single crystal, when irradiated with MgK_α X-rays emitted photoelectrons from various levels and also Auger electrons with periodically varying intensities at different angles between the axis of the crystal and the direction of electron emission. This phenomenon gave rise to a diffraction pattern which could be recorded in the instrument. This type of diffraction is different from the previously well-known electron diffraction when an external beam of electrons is diffracted in a crystal and which has been used extensively during recent years in LEED. It should be possible to explore the "ESCA Diffraction" under much improved conditions if higher intensities were available.

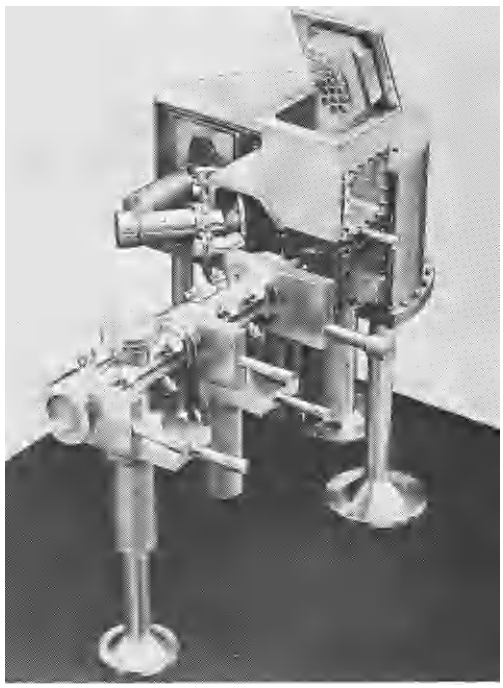

Fig. 42. Model of the new, optimized ESCA instrument. In the foreground: the three stage sample handling system. To the left: the rotating anode. Above: the multicrystal holder. Behind the sample house: the analyzer.

This survey will end with a brief discussion of new ESCA equipment[25] which has been under construction in our laboratory for some time. Figure 42 is a photo of a model of this instrument. One observes in the foreground the sample preparation system. The sample is introduced through this system in three subsequent steps with increasing vacuum until it is put into source position for running the electron spectrum under ultrahigh vacuum conditions. Several methods of preparations are available for the sample, like evaporation, sputtering, heating, gas reactions etc. The X-ray monochromator is in principle similar to the prototype instrument shown in Fig. 5 but of a much more powerful performance. The electron gun will run at a power level of 20 kW (100 mA and 20 kV). The watercooled rotating anode has a diameter of 30 cm and is designed for a speed of >20,000 rev/min. On the Rowland circle an assembly of 19 spherically bent quartz crystals ($\phi = 3$ cm) are mounted on a block of grinded glass and combine to give a minimum of spherical aberration and produce a monochromatic AlK_α line to within 0.18 eV. This radiation will hit the sample, a gas or a solid, from above, in front of and along the slit of a 22 cm long four-component electrostatic lens system under conditions designed to give minimum aberration and to provide a large reduction of the energy of the electrons (a retardation factor up to 30). The spherical analyzer has a mean radius of 36 cm and a separation of 15 cm between the spheres. A correspondingly long multidetector is placed in the focal plane. The inside volume of the instrument is provided with two shields of μ-metals. Overall the instrument is pumped by 3 separate He cryopumps and by two additional ones in the sample preparation system. Around the sample position there are further facilities for other modes of excitation like a He-lamp, $YM\zeta$-anode, electron gun and a monokinetic electron beam device. The system should be flexible enough to allow many experimental arrangements to be made. This instrument should primarily be used for gases, although solids can also be studied. A second instrument is simultaneously being built, primarily intended for solids, liquids and surfaces. In this case it is more advantageous to let the X-rays hit the sample from the side, i.e. perpendicular to the lens slit, and not along the slit as for the gas instrument. One can then use more crystals, (25), and thus increase the intensity of the monochromatic radiation. As a consequence of this design the rotating anode and the electron gun has to be situated where the sample handling system was in the previous case. The sample handling system for the latter instrument is placed to the right side of the source compartment house. In other respects the two instruments are identical. These two instruments are complex in design and require much careful adjustments for optimum performance. If they operate according to the calculations a large increase in intensity (>100) is obtained and much improved provisions for sample handling is attained.

REFERENCES

[1]K. Siegbahn, Electron spectroscopy—An outlook, *J. Electron Spectrosc.* **5**, 3 (1974); Conference Vol. edited by R. Caudano and J. Verbist, and references therein.

[2]R. Nilsson, A. Berndtsson, N. Mårtensson, R. Nyholm and J. Hedman, UUIP-913 (1975).

[3]O. Jepsen, O. Krogh Andersen and A. Mackintosh, *Phys. Rev.* **B**, (1975).

[4]B. Lindberg, S. Svensson, P. Å. Malmqvist, E. Basilier, U. Gelius and K. Siegbahn, UUIP-910 (1975).

[5]M. Krause, *Chem. Phys. Lett.* **10**, 65 (1971); M. Krause and F. Wuilleumier, *Phys. Lett.* **35A**, 341 (1971).
[6]M. Banna and D. Shirley, LBL-3478 and LBL-3479 (1975).
[7]D. Allison and R. Cavell, ACS April Meeting, 1975.
[8]R. Nilsson, R. Nyholm, A. Berndtsson, J. Hedman and C. Nordling, UUIP-912 (1975).
[9]J. W. Rabalais, T. Debies, J. Berkosky, J. Huang and F. Ellison, *J. Chem. Phys.* **61**, 516 (1974).
[10]L. Karlsson, L. Mattsson, R. Jadrny, R. Albridge, S. Pinchas, T. Bergmark and K. Siegbahn, *J. Chem. Phys.* **62**, 4745 (1975).
[11]L. Karlsson, L. Mattsson, R. Jadrny, T. Bergmark and K. Siegbahn, UUIP-911 (1975).
[12]D. Shirley, *J. Vac. Sci. Tech.* **12**, 280 (1975).
[13]C. Brundle and M. Roberts, *Proc. Roy. Soc. Lond.* **A331**, 383 (1972).
[14]D. Hercules, L. Cox, S. Onisick, G. Nichols and J. Carver, *Analyt. Chem.* **45**, 1973 (1973).
[15]D. Hercules, personal communication.
[16]H. Siegbahn, L. Asplund and P. Kelfve, *Chem. Phys. Lett.* **35**, 330 (1975).
[17]H. Ågren, S. Svensson and U. I. Wahlgren, *Chem. Phys. Lett.* **35**, 336 (1975).
[18]H. Siegbahn and O. Goscinski, UUIP-908 (1975).
[19]G. Howat and O. Goscinski, *Chem. Phys. Lett.* **30**, 87 (1975).
[20]H. Siegbahn, R. Medeiros and O. Goscinski, *J. Electron Spectrosc.* 7 (1975).
[21]H. Fellner-Feldegg, H. Siegbahn, L. Asplund, P. Kelfve and K. Siegbahn, *J. Electron Spectrosc.* **7**, 421 (1975).
[22]H. Siegbahn, L. Asplund, P. Kelfve, K. Hamrin, L. Karlsson and K. Siegbahn, *J. Electron Spectrosc.* **5**, 1059 (1974).
[23]H. Siegbahn, L. Asplund, P. Kelfve and K. Siegbahn, *J. Electron Spectrosc.* **7**, 411 (1975).
[24]K. Siegbahn, U. Gelius, H. Siegbahn and E. Olson, *Phys. Lett.* **32A**, 221 (1970); *Physica Scripta* **1**, 272 (1970).
[25]U. Gelius, H. Fellner-Feldegg, B. Wannberg, A. G. Nilsson, E. Basilier and K. Siegbahn, UUIP-855 (1974).